Structure and Isothermal Crystallization Behavior of Polypropylene Prepared at High Polymerization Temperature

Chifeng Zhong,[1] Bingquan Mao[2]

[1]*Research Center of Polymer Materials and Environmental Engineering, Dongguan University of Technology, Dongguan, Guangdong Province 523808, People's Republic of China*
[2]*Polyolfins National Engineering Research Center, Beijing Research Institute of Chemical Industry, SINOPEC, Beijing 100013, People's Republic of China*

Received 10 December 2008; accepted 11 May 2009
DOI 10.1002/app.30737
Published online 7 July 2009 in Wiley InterScience (www.interscience.wiley.com).

ABSTRACT: The structure, morphology, and isothermal crystallization behaviors of polypropylene (PP) prepared with heterogeneous Ziegler-Natta catalyst at high temperature (100°C) were investigated with differential scanning calorimetry, wide-angle X-ray diffraction, temperature-rising elution fractionation, gel permeation chromatography, and ^{13}C NMR. The results reveal that the crystalline structure changes with variation of the composition of the PP. The isotactic PP (iPP)1 prepared with Et_3Al and "TMA-depleted" methylaluminoxane crystallizes from the melt in the mixtures of the α and β forms, whereas each fraction obtained from pure PP1 does not show β-PP crystal at the same crystallization condition. In addition, the γ-PP crystal is appeared for the fractions of low mmmm%-[mmmm] (mmmm pentad content) values and molecular weight. Moreover, it was found that the iPP2 or iPP3 prepared with Hex_3Al crystallizes from the melt in mixtures of the α and γ forms, even at atmospheric pressure and for high molecular weight. The microstructure showed in the PP samples obtained at high temperature could be well explained with the shift in the alkylaluminium-donor equilibrium reactions at high polymerization temperature. © 2009 Wiley Periodicals, Inc. J Appl Polym Sci 114: 2474–2480, 2009

Key words: polypropylene; morphology; isothermal crystallization; structure

INTRODUCTION

Isotactic polypropylene (iPP) is a semicrystalline polymer widely used in industrial and commercial applications. Since the application on an industrial scale of Ziegler-Natta catalyst technology, many aspects of the morphology and mechanical properties of iPP and their relationships have been determined. The intrinsic polymer structure is related to the catalyst, polymerization, and compounding technologies. It is well recognized that heterogeneous Ziegler-Natta catalysts contain multiple active sites, which produce PP with varying degree of stereoregularity.[1–4] Despite considerable efforts with different analysis methods, it has not been possible to determine the exact structures of the reactive active sites. If the polymer characterization can be done thoroughly enough, information on the catalyst is gained as well. The most revealing information related to the catalyst and the polymerization mechanism of PP is the distribution of stereoerrors and stereoregular sequences in the formed polymer.

It is well known that the industrial polymerization temperature of $MgCl_2$-supported Ziegler-Natta catalysts are around 65–80°C.[3] In recent years, a new supercritical olefin polymerization technology was developed, which needed higher polymerization temperature (>90°C) for propylene polymerization. In our previous paper,[5] we have reported that the $TiCl_4/MgCl_2$/dibutyl phthalate(DNBP)-cylohexanemethyl dimethyloxysilane catalyst showed a high proportions of iPP and high activity with the mixture of "TMA-depleted" methylaluminoxane (MMAO) and Et_3Al at 100°C and the resultant PP exhibited bimodal peaks, and one was in the vicinity of 160°C and the other was in the vicinity of 150°C. In contrast, the PPs prepared with either *i*-bu_3Al or Hex_3Al at same polymerization conditions exhibited the only peak in the vicinity of 160°C. The peak at low temperature (150°C) may result from the formation of β-PP crystal.[5] It has been demonstrated by researchers that the presence of the β-form within the crystalline portion of the material is beneficial to its macroscopic toughness and ductility.[6,7]

Correspondence to: C. Zhong (zhongchifeng@yahoo.com.cn).
Contract grant sponsor: Dongguan Science and techonology Project ([2006]18).

The objective of this study is to elucidate the microstructure and morphology of PP obtained at high temperature using temperature-rising elution fractionation (TREF), ^{13}C-NMR, gel permeation chromatography (GPC), differential scanning calorimetry (DSC), and wide-angle X-ray diffraction (WAXD) analyses. This work is a continuation of our previous work[5] on studying propylene polymerization at high temperature. TREF is the most common method for obtaining detailed information about PP stereoregurality distribution.[8,9] In this study, the preparation and characterization of PP fractions and PPs are reported. Also, the growth mechanism of the β-PP and γ-PP crystals is discussed on the basis of the obtained results.

EXPERIMENTAL

Materials

The PP samples used in this investigation are synthesized in our laboratory, which follows the description given in Ref. 5. For these samples, the polymerization temperature is 100°C and the mixture of MMAO and Et_3Al (for PP1) or Hex_3Al (for PP2) or only Hex_3Al (for PP3) was added as the cocatalyst.

Fractionation and molecular weight and ^{13}C NMR characterization

The PP1 sample was fractionated using the same temperature-rising elution procedure in our preparative TREF equipment. The fractionation process is described as follows: 1 wt % PP1 sample was first dissolved in 1,2,4-trimethybenzene at 140°C, and then introduced into the elution column of TREF under the N_2. The process to precipitate PP onto the surface of the support was finished by cooling the polymer solution from 140 to 25°C in 85 h. The elution step was carried out with trimethylbenzene at 25, 80, 100, 105, 110, 120, and 140°C, respectively. The recovery of all the fractions was 98.4%.

The molecular weight of iPPs and all the TREF fractions was measured by a Waters GPC Alliance GPCV 2000. The weight-average and number-average molecular weight (M_w and M_n, respectively) of polymers were calculated on the basis of a polystyrene standard calibration. ^{13}C-NMR spectra of the iPPs and TREF fractions were recorded with a Bruker DMX 400 spectrometer operating at 100.6 MHz, on 10 mg/mL solutions in deuterated dichlorobenzene at 110°C. Condition: 10 mm probe; acquisition time, 5 s; relaxation time, 10 s; numbers of scans, 5000.

Crystallization and melting behavior characterization

The thermal analysis was carried out by means of DSC (Perkin-Elmer DSC-7) under the N_2. The samples of about 5 mg were heated to 200°C and held in the molten state for 5 min to eliminate the influence of thermal history. The sample melts was then subsequently quenched at a rate of 80°C/min to reach 125°C for isothermal crystallization for 60 min. Then, the sample was heated at 10°C/min again.

WAXD was obtained at room temperature with an automatic Philips diffractometer (X'Pert, MPD). The samples (8 mm radius and 1 mm thickness), which were covered with thin Al foil, was first immersed in a silicone oil bath at 200°C for 6 min and then quickly turned to another silicone oil bath at 125°C for 60 min. Then, the samples are cooled at room temperature.

RESULTS

As mentioned in the Introduction section, the $TiCl_4$/$MgCl_2$/DNBP-cylohexanemethyl dimethyloxysilane catalyst showed a high proportion of iPP and high activity with the mixture of MMAO and Et_3Al at 100°C and so the resultant PP1 was chosen for the fractionation. The characterization of iPPs are listed in Table I. The TREF results and characterization of the fractions are listed in Table II. For crystallization fractions, the molecular weight (M_w) increases with the increase in elution temperature. But for the fration F1 which is known as the atactic PP, it was found whose molecular weight was even higher than that of F5, even though it was only 2.4 wt %. This verified that the fractionation mechanism in TREF analysis is basically based on the longest crystallizable sequence rather than molecular weight, and the longer sequences determine the higher crystallization temperature of a molecular chain.

DSC melting traces of the iPP1 (heptane-insoluble fraction of PP1) sample and the fractions of PP1 after isothermal crystallization at 125°C are shown in Figure 1. The melting point and the enthalpy of fusion (ΔH_f) was also given in Table II. The iPP1 exhibited two melting peaks as shown in Figure 1,

TABLE I
The Characterization of iPPs

	Cocatalyst	T_m (°C)	ΔH_f (J/g)	$M_w \times 10^{-3}$ (g/mol)	M_w/M_n
iPP1	MMAO and Et_3Al	149.5, 161.6[a]	94.3	234	4.5
iPP2	MMAO and Hex_3Al	159.9	84.4	275	3.7
iPP3	Hex_3Al	159.5	81.8	331	4.1

[a] Double peaks.

TABLE II
TREF Results and Characterization of the Fractions of PP1

	T_{el} (°C)	wt (%)	T_m (°C)	ΔH_f (J/g)	$M_w \times 10^{-3}$ (g/mol)	M_w/M_n
F1	25	2.4	–	–	121	3.6
F2	26–80	7.6	[a]	0	79	7.4
F3	81–100	11.8	150.2	81.7	85	4.4
F4	101–105	6.1	154.1, 158.7[b]	101.1	99	3.6
F5	106–110	13.0	161.0	107.1	99	2.4
F6	111–120	58.9	164.7	105.7	342	3.4
F7	121–140	0.2	–	–	–	–

[a] No peak.
[b] Double peaks.

and one is in the vicinity of 160°C and the other is in the vicinity of 150°C, as previously reported in Ref. 5. The crystallization fraction F2 showed no peak as shown in Figure 1. It indicated that fraction F2 did not crystallize at 125°C. And, it was worth noting that fraction F3 also showed a melting peak in the vicinity of 150°C. For all the fractions obtained from the PP1 sample, the melting peak shifts to higher temperature with the increase in elution temperature.

To find out the exact crystalline structure of the iPPs and the fractions, WAXD was performed. The results of WAXD for the iPP1 and the fractions are displayed in Figure 2, and these results were obtained under the same experimental conditions. The full width half-maxium at 2θ angles of 14.0° of fractions obtained form WAXD decreased with the increase in elution temperature. It indicated that the crystallite size of the fractions increased with increase in elution temperature using the Scherrer's method.

It can be seen from Figure 2 that all of the most intense WAXD reflections at 2θ angles of 14.0°, 16.9°, 18.6°, 21.2°, and 21.9°, corresponding to the (110), (040), (130), (111) and (-131) lattice planes of the most common α-monoclinic structures, have appeared in the X-ray diffraction spectra of every sample. This indicated that in all cases the PP crystals grow dominatingly in their monoclinic α modification. As mentioned above, fraction F2 did not crystallize at 125°C. Considering the results obtained from WAXD, it indicates that the fraction F2 can crystallize when it cooled at room temperature from 125°C.

The characteristic peak at 16° was attributed to β modification (300) of PP and the intensity of the reflection at a 2θ of 20° was attributed to the characteristic of γ polymorph. As shown in Figure 2, it is worth noting that the iPP1 exhibited the characteristic peak at 16°, whereas this phenomenon for all the fractions of PP1 cannot be distinguished. And the peak of 16° was not seemed in the fraction F3 which showed a melting peak in the vicinity of 150°C in DSC analysis. On the other hand, the fraction F3 exhibited the characteristic peak at 20° which is associated with γ polymorph while this peak is not observed in the iPP1 sample. It indicated that a lower degree of perfection of γ-PP crystal coexists with α-PP crystal in fraction F3 during crystallization process.

The typical WAXD intensity pattern of α-PP crystal, the intensity of second peak (040) must be smaller than the first one peak (110).[10] The WAXD intensity curve of F2 showed an unusual pattern that the second peak (at 16.9°) is larger than the first one (at 14.0°). The characteristic peaks of the presence of γ-PP crystal usually can be found at 2θ angles of 13.8° (111), 15.1° (113), 16.7° (008), 20.1° (117), 21.2° (202), and 21.9° (026). These results indicated that the location of the strongest second peak may be due to the (008) of γ-PP crystal coexisting with the (040) of α-PP crystal, although the peak at 20.1° was not distinguished. It implied that a lower

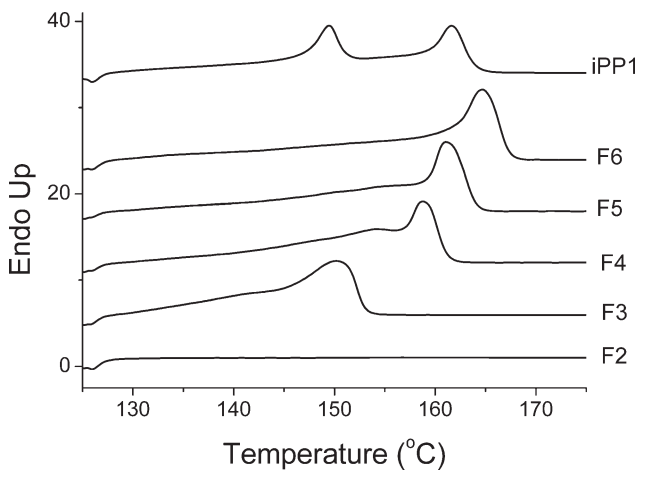

Figure 1 Comparison of melting curves subsequent to crystallization at 125°C for 60 min, heating rate is 10°C/min.

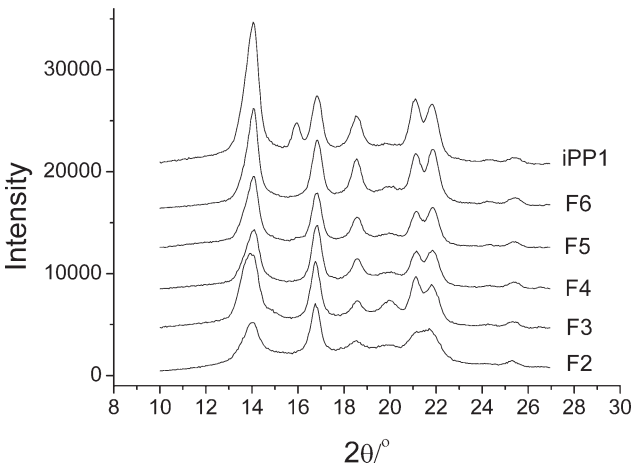

Figure 2 The WAXD evidence of β modification for iPP1 and γ modification for F3 and F2. The experiments were conducted under the same condition: after holding 200°C for 6 min, quickly turning the sample to a hot bath at 125°C for 60 min.

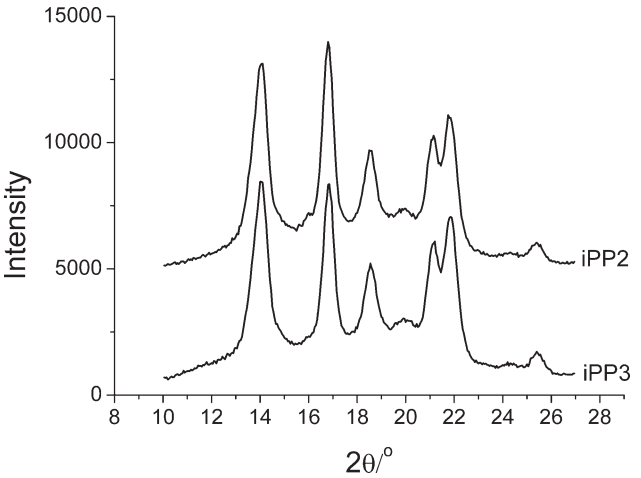

Figure 3 The WAXD evidence of γ modification for iPP2 and iPP3, as previously reported in Ref. 5. Crystallization condition: after holding 200°C for 6 min, quickly turning the sample to a hot bath at 125°C for 30 min.

degree of perfection of γ-PP crystal coexists with α-PP crystal during fraction F2 crystallization from 125°C to room temperature.

The result of WAXD for the iPP2 (heptane-insoluble fraction of PP2) and iPP3 (heptane-insoluble fraction of PP3), which were synthesized with Hex_3Al as the cocatalyst at high temperature, is also displayed in Figure 3. Although these WAXD patterns were already available in the literature,[5] it is discussed here in greater detail. These patterns are same as that of the fration F2, which were characterized by that the second peak is higher than the first one. And, in these WAXD patterns a small peak of γ-form (117) at 2θ angle of 20.1° was found. As discussed earlier, the result of WAXD confirmed that the iPP2 or iPP3 crystallizes in the α and γ form, even at atmospheric pressure and for high molecular weight.

The ^{13}C-NMR analysis was then conducted to obtain information on the microstructure of the selected samples. The pentad distributions of these fractions and iPPs, which were calculated from the methyl region resonance, are listed in Table III. As shown in Table III, the [mmmm] pentad content of the fractions of PP1 increased with increasing elution temperature. Considering the DSC results, the melting point of fractions increased with increasing the [mmmm] value. Taking the GPC result into account, it verified that the PP tacticity strongly differs from the change in molecular weight. The fraction with lower weight has a lower isotacticity, and the fraction with large molecular weight has a higher isotacticity. As shown in Tables I and III, the melting point of iPP2 or iPP3 was clearly lower than that of iPP1, whereas the [mmmm] pentad content of iPP3 is lower than that of iPP1.

The ^{13}C-NMR spectra of fractions were shown in Figure 4. The spectra of the fraction F2 and F3 showed a number of small irregular peaks. Since the molecular weight of the F2 and F3 was low enough, the terminal groups of these PPs were also found in ^{13}C-NMR spectra.[11] However, peaks that are assigned to tail to tail or 1,3-combination were not found in the spectrum of F3 or F2. Therefore, the possible stereodefect of these fractions was only the opposite insertion of monomers.

DISCUSSION

Multiple melting behaviors of iPP1

The multiple melting behavior of pure PP sample, which depends on thermal conditions of crystallization, has been reported by many researchers.[1,2,12] Taking the DSC and WAXD results into account, the melting peak at about 150°C for the sample iPP1 should be associated with the melting of β modification of iPP1. It accords with literatures that the melting peak of β-PP was found to be in the 145–150°C interval.[2,12] It is worth noting that the melting peak of fraction F3 was also found to be about 150°C. And the fraction F4 exhibited two melting peaks; one at low temperature (154.1°C) and the other at high temperature (158.7°C). However, it can be clearly seen from Figure 2 that the characteristic peak at 16° attributed to β modification of F3 of F4 was nonexistent. It indicated that the peak of 150°C for the fraction F3 or the peak of 154.1°C for the fraction F4 was attributed to α-PP crystal of lower degree of perfection rather than β-PP crystal.

The formation of γ-PP and β-PP

It is well known that the iPPs obtained with heterogeneous Ziegler-Natta catalytic systems, under the

TABLE III
Steric Pentad Composition of iPPs and Fractions

	mmmm	mmmr	rmmr	mmrr	Mmrm+rmrr	rmrm	rrrr	rrrm	mrrm
F2	63.8	11.8	0.8	10.0	3.5	0.7	2.4	3.1	3.9
F3	82.5	6.7	0.5	4.8	1.6	0.3	0.6	1.0	2.0
F5	92.0	3.5	0.4	1.7	1.0	0.1	0.2	0.4	0.7
iPP1	91.6	3.0	0.1	2.5	0.8	0	0.4	0.6	1.0
iPP3	86.7	4.6	0.3	3.4	1.5	0.1	0.9	1.2	1.3

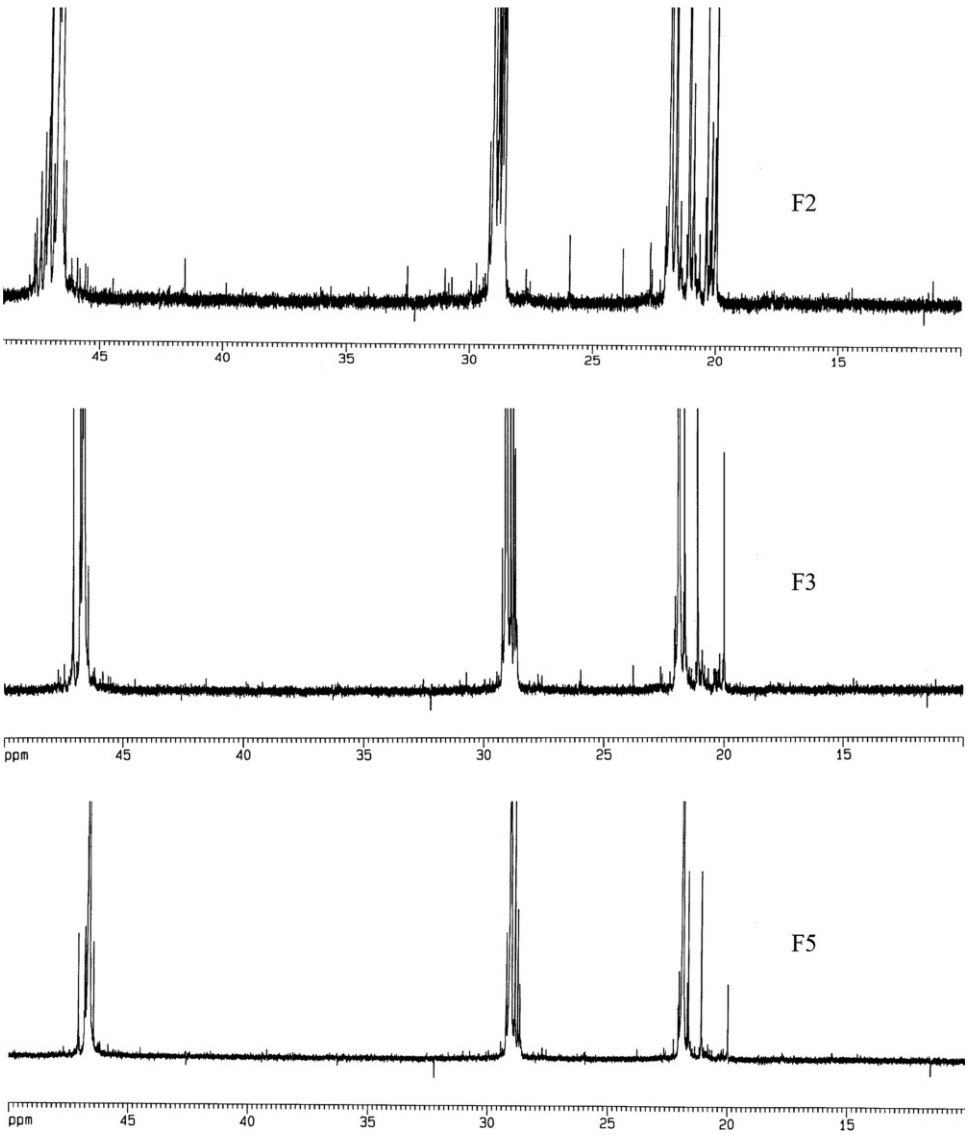

Figure 4 ^{13}C-NMR spectra of the fractions samples F2, F3, and F5.

most common conditions, crystallizes in the stable α form. As mentioned earlier, the more stereoregular fractions such as F5 and F6 crystallized instead basically in the α form. However, the fraction F2 and F3 crystallized from the melt in mixtures of the α and γ forms. Taking the ^{13}C-NMR and GPC results into account, it confirmed that short isotacitic sequences in low molecular weight fractions are in favor of the formation of γ modification. These results are in accordance with the study reported by other researchers.[1,2]

However, the iPP2 of weight-average molecular weight of 275,000 g/mol also crystallized from the melt in mixtures of the α and γ form, so did iPP3 of 331,000 g/mol. It was generally accepted that iPP samples prepared with homogeneous metallocene catalysts crystallizes more easily in the γ form, even at atmospheric pressure and for high molecular weight samples.[13]

Taking the ^{13}C-NMR results given in Table III into account, the average length of a continuous m sequence can be estimated from eq. (1)[14] if the pentad of mmmr is considered only.

$$\text{The average meso run length} = \text{MRL} = 2[\text{mmmm}]/[\text{mmmr} + \text{rmmm}] \quad (1)$$

The F2 or F3 contained high content of atactic pentads rmrm, rrrm, and rrrr. The iPP3 contained higher content of rrrm and rrrr than F3, even though

$$\text{C*·IED} + \text{AlEt}_3 \rightleftharpoons \text{C*} + \text{IED·AlEt}_3$$

$$\text{C*·EED} + \text{AlEt}_3 \rightleftharpoons \text{C*} + \text{EED·AlEt}_3$$

(C*: active site; IED: internal electron donor; EED: external electron donor.)

Scheme 1 Equilibrium reactions between $AlEt_3$ and electron donors.

the content of mmmm of iPP3 is higher than that of F3, as shown in Table III. The MRLs for iPP3 and the fraction F3 and F2 were 38, 25, and 11, respectively. It confirmed that short isotacitic sequences are in favor of the formation of γ modification. These analyses allowed concluding that the PPs prepared at high polymerization temperature are characterized by chains with a stereoblock microstructure, consisting of isotactic sequences linked to atatic (or more stereoirregular) sequences.

Sacchi et al.[15] proposed some equilibrium reactions existed in the PP polymerization reaction, shown in Scheme 1. They suggested that electron donors coordinating with active sites could be removed by $AlEt_3$ during the polymerization process and they also suggested that these reactions were reversible. Xu et al.[16] suggested that the equilibrium reactions between $AlEt_3$ and electron donors or between $AlEt_3$ and active sites are responsible for the formation of stereoblock structures.

When active sites coordinate with the electron donor and $AlEt_3$, they are more steric and produce more mmmm structures, whereas stereodefect structures are produced by the active sites without the donor.[15,16] Our previous study[17] comes to a conclusion that the electron donor can be removed more easily from the catalyst when polymerization temperature increases from 70 to 100°C. It implied that these equilibrium reactions between $AlEt_3$ and electron donors could shift to the right when polymerization temperature increases from 70 to 100°C. Therefore, this shift may lead to increase more stereoblock structure in the PP chain.

Being thermodynamically less stable than the α phase, the β phase can only be formed under specific conditions, such as temperature gradient, selective β-nucleating agents, and melt shearing.[1,2] Studies on the blends of PP with various copolymers demonstrated that copolymer components, such as ethylene–propylene copolymer[12,18] and ethylene–propylene–diene terpolymer,[19] are in favor of the formation of β-PP crystals. Li et al.[20,21] suggested that the orientation status of the PP chains in the melting state plays a leading role in generating the β-PP crystal.

On the basis of the above results, the origin on the formation of β-PP crystal in the iPP1 sample can be discussed. First of all, it can be definitely concluded that the formation of β-PP crystal in our case is associated with crystallization condition. In our study, the WAXD result showed that the β phase cannot be found and only α phase can be found when the iPP1 sample was quenched from 200°C to room temperature. Chaffin et al.[22] proposed that entanglements are the most important molecular factor in determining polymer properties in the melt and solid states and interfacial polymer entanglements, established in the molten state and subsequently anchored in chainfolded lamellae upon crystallization, influence polymer intrinsic properties. Rastogl et al.[23] proposed entanglements influence the polymer melt state and the resulting crystallization behavior. Therefore, taking the fact into consideration that β-PP has been generated in the pure iPP1 sample rather than all the fractions of PP1 sample separated by crystallization and elution process under the same crystallization conditions, the formation of β-PP in the iPP1 sample should result from the cooperative interaction between stereoblock fraction and highly isotactic fractions. In the other hand, it is worth noting that the fraction F6 (58.9 wt % of iPP1) has a melting point of 164.7°C while the iPP1 only has a melting point of 161.6°C at the same crystallization condition. The crystallite size of the fraction F6 is larger than that of iPP1 using the Scherrer's method. The result shows that the cooperative interaction of stereoblock and highly isotactic molecules could retard the thickening of the PP lamellae. These results implied that the cooperative interaction, such as blends or entanglements, of PP molecules of different isotacticities lead to an essential change in the structure of PP from α-PP to β-PP.

CONCLUSIONS

The structure, morphology, and isothermal crystallization behaviors of PPs obtained with heterogeneous Ziegler-Natta catalyst at high temperature (100°C) as well as its fractions were investigated. The PP1 prepared with Et_3Al as cocatalyst crystallized was characterized by the appearance of α-PP and β-PP crystals coexisting while each fraction obtained from PP1 did not show β-PP crystal at the same crystallization condition. In addition, the γ-PP crystal was appeared for the fractions of low mmmm% value and molecular weight. The high molecular weight PP2 and PP3 samples prepared with Hex_3Al as cocatalyst also crystallized from the melt in mixtures of the α and γ forms. This analysis allows concluded that the PPs prepared at high polymerization temperature are characterized by chains with a stereoblock microstructure, consisting of isotactic sequences linked to atatic (or more stereoirregular) sequences. The microstructure shown in the PP samples obtained at high temperature could be well explained with the shift in the alkylaluminium-donor equilibrium reactions at high polymerization temperature. Considering the detailed analysis of results, it was suggested that cooperative interaction of PP molecules of different isotacticities plays an important role in the formation of β-PP.

The authors acknowledge Dr. Mingzhi Gao for his support during the work.

References

1. Phillips, R. A.; Wolkowicz, M. D.; Moore, E. P., Ed. Polypropylene Handbook, Hanser/Gardner Publications: 1996; 126–170.
2. Bruckner, S.; Meille, S. V.; Petraccone, V.; Pirozzi, B. Prog Polym Sci 1991, 16, 361.
3. Barbe, P. C.; Cecchin, G.; Noristi, L. Adv Polym Sci 1987, 81, 1.
4. Alamo, R. G.; Blanco, J. A.; Agarwal, P. K.; Randall, J. C. Macromolecules 2003, 36, 1559.
5. Zhong, C.; Gao, M.; Mao, B. J Mol catalyst A Chem 2006, 243, 198.
6. Kotek, J.; Raab, M.; Baldrian, J.; Grellmann, W. J Appl Polym Sci 2002, 85, 1174.
7. Karger-Kocsis, J.; Varga, J.; Ehrenstein, G. W. J Appl Polym Sci 1997, 64, 2057.
8. Morini, G.; Lbizzati, E. A.; Balbontin, G.; Mingozzi, I.; Sacchi, M. C.; Forlini, F.; Tritto, I. Macromolecules 1996, 29, 5770.
9. Xu, J.; Fu, Z.; Fan, Z.; Feng, L. Eur Polym J 2002, 38, 1739.
10. Chen, J. H.; Tsai, F. C.; Nien, Y. H.; Yeh, P. H. Polymer 2005, 46, 5680.
11. Zhong, C.; Gao, M.; Mao, B. J Appl Polym Sci 2003, 90, 3980.
12. Zheng, Q.; Shangguan, Y.; Yan, S.; Song, Y.; Peng, M.; Zhang, Q. polymer 2005, 46, 3163.
13. Rosa, C. D.; Auriemma, F.; Circelli, T.; Waymouth, R. M. Macromolecules 2002, 35, 3622.
14. Randall, J. C.; Alamo, R. G.; Agarwal, P. K.; Ruff, C. J. Macromolecules 2003, 36, 1572.
15. Sacchi, M. C.; Tritto, I.; Locatelli, P. Prog Polym Sci 1991, 16, 331.
16. Xu, J.; Feng, L.; Yang, S. Macromolecules 1997, 30, 2539.
17. Zhong, C.; Gao, M.; Mao, B. Macromol Chem Phys 2005, 206, 404.
18. Karger- Kocsis, J.; Kallo, A.; Szafner, A.; Bodor, G.; Senyei, Z.. Polymer 1979, 20, 37.
19. Ha, C. J Appl Polym Sci 1988, 35, 2211.
20. Li, H.; Jiang, S.; Wang, J.; Wang, D.; Yan, S. Macromolecules 2003, 36, 2802.
21. Li, H.; Zhang, X.; Kuang, J.; Wang, J.; Wang, D.; Li, L.; Yan, S. Macromolecules 2004, 37, 2847.
22. Chaffin, K. A.; Knutsen, J. S.; Brant, P.; Bates, F. S. Science 2000, 288, 2187.
23. Rastogl, S.; Lippits, D. R.; Peters, G. W. M.; Graf, R.; Yao, Y.; Spiess, H. W. Nat Mater 2005, 4, 635.